Computers and Electronics in Agriculture 69 (2009) 158–164

Contents lists available at ScienceDirect

Computers and Electronics in Agriculture

journal homepage: www.elsevier.com/locate/compag

Classification of toxigenic and atoxigenic strains of *Aspergillus flavus* with hyperspectral imaging

Jian Jin[a], Lie Tang[a,*], Zuzana Hruska[b], Haibo Yao[b]

[a] *ABE, Iowa State University, United States*
[b] *GRI, Mississippi State University, United States*

ARTICLE INFO

Article history:
Received 25 March 2009
Received in revised form 22 July 2009
Accepted 30 July 2009

Keywords:
Hyperspectral image
Classification
Toxigenic and atoxigenic
A. flavus
Aflatoxin reflectance
Support Vector Machine
Principal component analysis
Genetic Algorithm
Bhattacharyya Distance

ABSTRACT

Aspergillus flavus (*A. flavus*) produces secondary metabolites, aflatoxins, that are harmful to both humans and animals. Because of stringent federal regulation requirements as well as the limitations of available detection methods, there is an urgent need for rapid, non-invasive and effective techniques such as hyperspectral imaging, for the detection of the toxigenic strains of *A. flavus*. Hyperspectral images of toxigenic and atoxigenic strains of *A. flavus* were classified. Principal component analysis (PCA) was applied for data decorrelation and dimensionality reduction. A Genetic Algorithm (GA) was implemented for the selection of principal components (PCs) based on Bhattacharya Distance (B-Distance). A Support Vector Machine (SVM) was successfully applied for the classification. Under halogen light sources, in average 83% of the toxigenic fungus pixels and 74% of the atoxigenic fungus pixels were correctly classified; while under UV light sources, 67% of the toxigenic fungus pixels and 85% of the atoxigenic fungus pixels were correctly classified. The pair-wise classification accuracies between toxigenic AF13 and each atoxigenic fungus species (AF38, AF283 and AF2038) were 80%, 91% and 95% under halogen light sources, and 75%, 97% and 99% under UV lights, respectively.

Published by Elsevier B.V.

1. Introduction

Mycotoxins are toxins produced by fungi, which are commonly found in food products. Aflatoxin is a type of mycotoxin and is harmful to humans as well as animals. It is a secondary metabolite produced by *Aspergillus flavus* (*A. flavus*) under drought stress and hot weather conditions. The main impact of non-toxigenic *A. flavus* strains on agriculture is in saprophytic degradation of grains both before and after harvest. Of more imminent concern is the impact on health caused by toxigenic, aflatoxin-producing strains of *A. flavus*. Contamination of food and feed grains with aflatoxin can cause potentially fatal human and animal diseases. In the United States, federal regulations limit aflatoxin concentrations in food for human consumption to 20 ppb and in animal feed to 100 ppb (USDA, 2002). There is thus an urgent need for rapid and reliable techniques to detect toxigenic strains of *A. flavus*.

Several screening methods for direct visual determination of aflatoxin production have been developed (Adye and Mateles, 1964; Davis et al., 1987; Dyer and McCammon, 1994; Torrey and Marth, 1976). These methods use complicated culture media containing additives to enhance the production of aflatoxins in order to achieve direct visual determination of a bright blue or blue-green fluorescent area surrounding colonies under UV radiation. However, the culturing conditions of these methods for the cultural media make them unsuitable for the determination of the aflatoxins developed under normal conditions.

More recently, spectrally based non-invasive techniques for mycotoxin detection were developed. Two techniques, photoacoustic spectroscopy (PAS) and diffuse reflectance spectroscopy (DRS), were coupled to a Fourier transform infrared (FTIR) spectrometer to provide information about the mid-infrared absorption spectra of corn (Greene et al., 1992). Spectra generated from corn infected with mycotoxin were found to be dramatically different from those of uninfected corn. A pattern recognition program with FTIR-PAS was used to detect *A. flavus* and other toxigenic fungal contamination present in food grains, and the classification accuracy rates were 96% for positives and 84% for negatives (Gordon et al., 1998). However, these techniques with FTIR have a limited potential because the photoacoustic detectors can accommodate only a single kernel at a time. Transient infrared spectroscopy (TIRS) is a technique for online, noncontact detection of *A. flavus*, which is potentially effective in screening bulk quantities of corn grain (Gordon et al., 1999). Early tests based on visual inspection of TIRS spectral differences had an accuracy

* Corresponding author at: Agricultural and Biosystems Engineering, Iowa State University, 203 Davidson Hall, Ames, IA 50011, United States. Tel.: +1 515 294 9778; fax: +1 515 294 2255.
E-mail address: lietang@iastate.edu (L. Tang).

0168-1699/$ – see front matter. Published by Elsevier B.V.
doi:10.1016/j.compag.2009.07.023

rate between 85% and 95% in distinguishing healthy corn kernels from infected ones. The limitation of TIRS is the special requirements on heating the media surface for producing proper thermal emission.

Hyperspectral imaging techniques which capture a set of images over a range of wavelengths are also candidates for such applications. They overcome the shortcomings of the above screening techniques by having the advantages of quick and untouched image screening, capturing large quantity of pixels simultaneously, and being compatible to various culturing conditions. The disadvantage of the current spectrometer system compared with hyperspectral imaging is the coverage uncertainty of its targeted field of view. For a hyperspectral image, image spatial information such as pixel location can be used in the process of defining regions of interest (ROI), and the target pixels within ROI can be clearly identified. Hyperspectral imaging techniques have been successfully applied for classification of agricultural products, including defect detection on apples (Ariana et al., 2006), cherries (Guyer and Yang, 2000) and cucumbers (Cheng et al., 2004).

Hyperspectral imaging has a great potential to be applied to *A. flavus* fungal strain classification. Recent experiments using hyperspectral imaging techniques identified a unique spectral signature for *A. flavus* that is readily identifiable against any background or surrounding surface and among other fungal strains (DiCrispino et al., 2005). Pearson and Wicklow (2001) utilized transmittance spectra (500–950 nm) and reflectance spectra (550–1700 nm) to detect aflatoxin contamination in corn kernels. For both cases, more than 95% of the kernels were correctly classified as containing either high (>100 ppb) or low (<10 ppb) levels of aflatoxin.

The classification between toxigenic and atoxigenic strains of *A. flavus* is more difficult due to their close genetic relationship. A molecular method of using a dual step DNA fingerprinting approach was found to be potentially effective in resolving toxigenic from non-toxigenic *A. flavus* strains, if more markers of the genome of *A. flavus* were known (Baird et al., 2006). As for the spectral-based approach, to the best of our knowledge, no attempt has been made in classifying toxigenic and atoxigenic strains of *A. flavus*.

The overall objective of this research was to develop a classification algorithm to classify hyperspectral images of toxigenic and atoxigenic strains of *A. flavus* and evaluate the performance of the developed algorithm. It was also studied whether each of the four *A. flavus* species was distinguishable from the others.

2. Materials and methods

2.1. Experiments and imaging

Aflatoxin-producing *A. flavus* (AF13) plus three non-toxin-producing *Aspergillus* strains (AF2038, AF283 and AF38) were obtained from and cultured at the Food and Feed Safety Laboratory, SRRC, USDA, New Orleans, LA. Three replicates of each of the four AF strains were cultured on potato dextrose agar (PDA) medium at room temperature (25 °C) for 7 days, in the dark. To seed the fungi, 10 μl of culture stock, at a dilution of 4 × 106 spores/ml from each fungal strain, was introduced to the center of the medium in each dish with a pipette.

Two separate hyperspectral imaging configurations were used to acquire images. The first set of images was taken for reflectance measurement using two mr16 tungsten halogen bulbs with dichroic reflectors. The second set of images was taken for fluorescence measurement with a deuterium broad spectrum UV light source. UV light was used to explore the potential of using fluorescence responses of *A. flavus* for this application. The UV light source was a 200 W deuterium lamp (Heraeus, MS Scientific, Germany) that generates a continuous spectrum in the wavelength range from 160 nm to 400 nm in a vacuum and 180 nm to 400 nm in air.

A visible/near infrared (VNIR) hyperspectral sensor (VNIR-100E, Institute for Technology Development, MS) was used for image data acquisition. The VNIR-100E uses a line scanning technique that eliminates the requirement of a mobile platform in a pushbroom hyperspectral scanning system. The system uses a technique called focal plane scanning (US Patent No. 6,166,373) which moves the lens within the camera system. Image data was acquired with a 12-bit CCD camera with a 1376 × 1040 pixel CCD sensor in which the 1376 axis is for the spatial dimension and the 1040 axis is for spectral dimension. Image data was captured using variable binning to allow image acquisition at user specified spatial and spectral resolutions. In this study, the spatial and spectral binning was 2 and 4, respectively. Thus the 2 × 4 binning on a 1376 × 1040 CCD resulted image size of 688 × 260 pixels per line. The sample image had 525 lines. The resulting output image contained a reflectance spectrum from 400 nm to 1000 nm with spectral resolution of 2.43 nm. The spectral resolution was the spectral channel interval of adjacent bands.

All samples were imaged in random order under two different imaging conditions described above. As each setup requires specific conditions, all dishes were first imaged using the halogen light source, before acquiring images with the second setup using the UV light source.

2.2. Image pre-processing

The raw images were first pre-processed using a series of steps described previously (Hruska et al., 2005). As in Hruska's work, a series of pre-processing steps were applied to each raw hyperspectral image in batch mode: (1) geometric correction; (2) data format conversion; (3) scene calibration to percentage reflectance; (4) wavelength assignment; (5) noisy band removal. Geometric correction rotated the image to the correct image orientation. Data format conversion converted image data from two-byte integers to floating point numbers. Scene calibration converted data to standard reflectance. Wavelength assignment set each image band with its appropriate wavelength. Due to their relatively high levels of background noise, image bands from 400 nm to 450 nm and 900 nm to 1000 nm were discarded during the noisy band removal step. In scene calibration, a dark and a reference scan were used to convert the raw digital counts to percent reflectance. The dark image data was taken with the camera lens completely blocked. The reference scan was taken over a standard diffuse reflectance surface (Spectralon: SRT-99-100 UV-VIS-NIR Diffuse Reflectance Target, LabSphere Inc.). The following equation was used in the calibration:

$$Reflectance_\lambda = \frac{S_\lambda - D_\lambda}{R_\lambda - D_\lambda} \times 100\% \quad (1)$$

where $Reflectance_\lambda$ is the reflectance at wavelength λ; S_λ was the sample intensity at wavelength λ; D_λ was the dark intensity at wavelength λ; R_λ was the reference intensity at wavelength λ. After pre-processing, the calibrated image had 184 bands ranging from 450 nm to 900 nm. The integration time for the white reference, dark, and sample images was all the same.

To identify the spectral signature of mature *A. flavus*, reflectance values were obtained through a spatial subset of the image (region of interest) along with standard deviation. Similar spectral intensity signatures of the pixels from the hyperspectral images of toxigenic and atoxigenic strains of *A. flavus* were observed (e.g., Fig. 1). Meanwhile, variance was evident among the pixels from the same fungal species as well. Therefore, to identify the spectra of different *A. flavus* strains, advanced classification techniques were needed.

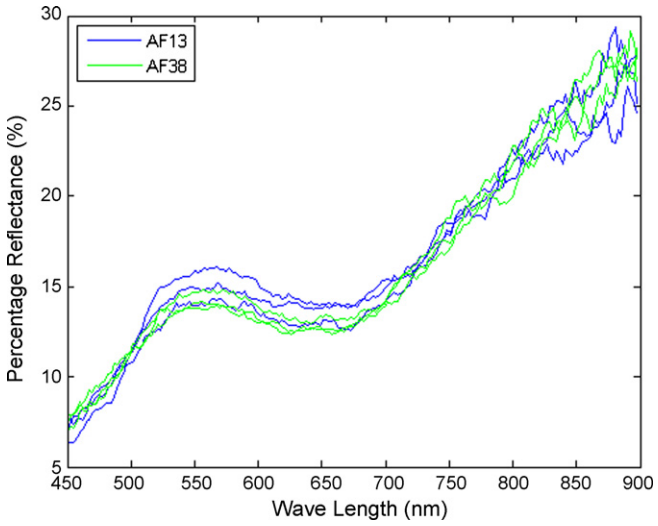

Fig. 1. Spectrum of three sample pixels in AF13 and AF38 hyperspectral images.

2.3. Spectral angle-based filtering

In the experiments, the spectra of aflatoxin-producing *A. flavus*, AF13, needed to be classified from each of the three non-toxin producing *Aspergillus* strains, AF2038, AF283 and AF38. First, the fungal pixels needed to be selected to exclude the pixels representing agar. The *R* (Band # 82 at 650 nm), *G* (Band # 25 at 510 nm), and *B* (Band # 11 at 475 nm) bands of an AF13 image were used to form a *RGB* color image of each strain sample, in which an outer blue circle was formed where the agar was located in the Petri dish and a cloud-like green area was formed in the middle of the dish where the fungal colony grew (Fig. 2). The darker center of this green cloud is the inoculation spot. The region of interest (ROI) is within the fungal colony, excluding the inoculation spot in the center.

The outlier spots and pixel with differing spectra than the mean spectral fungal pixels, called noise pixels, exist within the mold colony (Fig. 2). The reliability of the final classification results is dependent on the exclusion of these noisy pixels. Segmentation based on spectral angles was implemented for the noise removal. First, the mean intensity values of the pixels in a chosen ROI were calculated on *R* (650 nm), *G* (510 nm), and *B* (475 nm) bands. These average intensity values formed a three-dimensional vector, namely a mean vector. For each selected pixel, a three-dimensional *RGB* vector consisting of its *R*, *G*, *B* values was also formed. Then, the spectral angle between each selected pixel's *RGB* vector and the average *RGB* vector was calculated as follows:

$$SA = \arccos\left(\frac{RGB_P \cdot RGB_A}{\left\|RGB_P\right\| \cdot \left\|RGB_A\right\|}\right) \quad (2)$$

where SA = spectral angle; RGB_P = a three-dimensional vector consisting of the *R*, *G*, *B* values of a pixel; RGB_A = a three-dimensional vector consisting of the average *R*, *G*, *B* values of a chosen ROI.

Since the angle between a noisy pixel's *RGB* vector and the average *RGB* vector was assumed to be large, only the pixels having spectral angles smaller than a threshold of 0.01 rad were kept for the classification process.

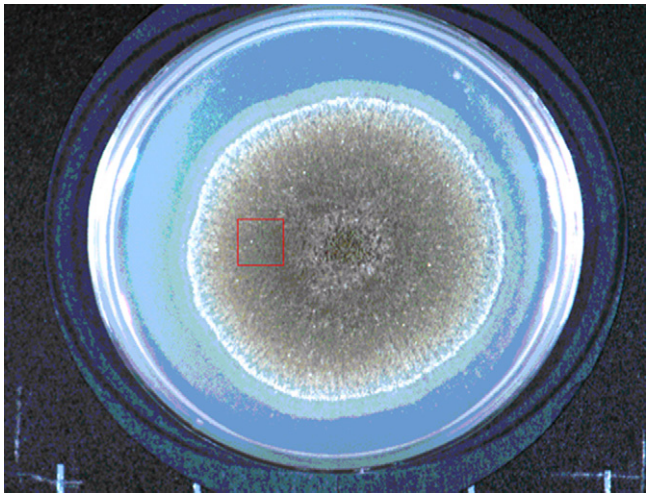

Fig. 2. The *RGB* color image of an AF13 sample under halogen lights. The darker center of this green cloud is the inoculation spot. The square is an example ROI.

2.4. Multivariate analysis of variance

The differences in lighting and so on between different replicates may interfere in the classification. Multivariate analysis of variance (MANOVA) was conducted on the pixels from the three replicates of each AF strain to confirm there were no significant differences between means of the data from the three replicates. There were 1500 pixels randomly selected from the ROIs in each replicate. After the segmentation based on spectral angle, 200 pixels from each replicate were sent to MANOVA.

2.5. Principal component analysis

As the number of spectral bands becomes large, the limitation on the capability of detecting classes can become severe (Luis and Landgrebe, 1998). It has been estimated that as the number of dimensions increases, the training sample size needs to increase exponentially in order to keep the same performance of a non-parametric classification (Scott, 1992; Hwang et al., 1994). These limitations are what have been called the curse of dimensionality (Duda and Hart, 1973), and principal component analysis (PCA) can be used for the dimensionality reduction.

PCA is mathematically defined as an orthogonal linear transformation that transforms the data to a new coordinate system (Pearson, 1901). PCA is commonly used before feeding the data into any classification scheme. There are two general purposes of using PCA: dimensionality reduction and data decorrelation. In hyperspectral data processing for pattern recognition, the hyperspectral data stack can be composed of more than a hundred of spectral bands, which are usually heavily correlated. In this application, PCA was used for data decorrelation as well as for identifying the bands of the most significant influence to the classification. Several lowest order PCs were selected from the 184 dimensional hyperspectral data and the number of selected PCs was initially determined by checking the 'Scree Plot' which plots the eigenvalues of PCs in a descending order.

2.6. PC bands selection using Genetic Algorithm

When most data variance needs to be retained, it is often difficult to reduce data dimensionality by only checking the 'Scree Plot' because a large number of lowest order PCs often need to be kept. The lowest PCs contain the greatest variance of data, which often result in easier classification. However, the maximum separation between classes cannot be guaranteed by simply selecting the lowest PCs. Therefore, it is necessary to search for a combination of PCs that can lead to the maximum separation between the classes. An exhaustive search was first applied to find such a combination. However, the number of possible PC combinations and the corresponding search time increases exponentially with the increase

of selectable PCs, easily making the greedy search method computationally infeasible. For instance, the exhaustive search among the 15 lowest order PCs cost about half an hour to compute on a computer with 4-core 3.2 GHz Intel Xeon CPU. Therefore, instead, Genetic Algorithm (GA) was implemented to search for combinations among the first 40 PCs (which explained more than 95% of the total variance). GA was selected for this purpose with two reasons. First, the combination of PCs can easily be represented by binary chromosomes. Second, GA is regarded as a proper method for searching for an optimal combination within a very large search space, which would cost a long time for greedy search method.

When using GA, it is important to set up proper configuration values such as population size, crossover and mutation rates. These GA components and operators settings are described below.

2.6.1. Chromosome

The GA was used to search for the PC combination among the 40 lowest order PCs with the highest B-Distance. Therefore, a 40-bit binary string was used to represent the selection among the 40 PCs for each PC combination.

2.6.2. Population size

Goldberg's (1989b) rule of thumb calls for a population size approximately equal to the chromosome length. Therefore, a population size of 50 was first used. However, it was observed that in this application, the individuals from the whole population tended to converge to the same chromosome after several generations of evolution. Since the variability among the individuals of the same generation is critical to the evolution, a much larger population size of 200 was used.

2.6.3. Selection

Local tournament selection without replacement with a size of four was implemented. It was chosen over roulette wheel selection because the latter could cause premature problems at earlier stages (Tang et al., 2000).

2.6.4. Fitness

Bhattacharyya Distance (B-Distance) was adopted as the criterion for the PC selection. The B-Distance (Bhattacharyya, 1943) is defined as:

$$BD = \frac{1}{8}(m_i - m_j)^t \left(\frac{\Sigma_i + \Sigma_j}{2}\right)^{-1} (m_i - m_j) + \frac{1}{2}\ln\left(\frac{\left|(\Sigma_i + \Sigma_j)/2\right|}{\left|\Sigma_i\right|^{1/2}\left|\Sigma_j\right|^{1/2}}\right) \quad i, j = 1, 2, 3 \tag{3}$$

where m_i and m_j are means of the training classes i and j; Σ_i and Σ_j are the covariances of these training classes. B-Distance is normally used to measure the separability of classes in classification problems, and was successfully applied to a texture segmentation problem (Reyes-Aldasoro and Bhalerao, 2006). In another application of using hyperspectral imaging for soil nutrient mapping (Yao et al., 2003), GA was used to select a group of bands. These selected bands were then used for PCA; and two PC bands that produced the highest B-Distance were finally selected for classification. However, when there are large number of bands, applying PCA before GA is helpful in reducing the searching space for GA, therefore eliminates the omission of any critical bands.

2.6.5. Crossover and mutation

De and Kenneth (1975) showed that good GA performance requires a high crossover probability. Therefore a crossover probability of 0.8 was adopted. Goldberg (1989a) recommended a mutation rate inversely proportional to the population size. However, because of the early convergence problem mentioned above, apart from using a larger population size, a larger mutation rate of 0.08 was selected.

2.7. Configuration of SVM

Advanced classification techniques were required to differentiate the spectral signatures of toxigenic and atoxigenic strains of *A. Flavus*. Computational intelligence (CI) techniques have been widely used to for this kind of difficult classification applications. Among various CI techniques, the Support Vector Machines (SVM) marked the beginning of a new era in the "learning from examples" paradigm. Rooted in Statistical Learning Theory (Vapnik, 1995), SVMs quickly gained attention from the pattern recognition community due to a number of theoretical and computational merits, including the simple geometrical interpretation of the margin, uniqueness of the solution, statistical robustness of the loss function, modularity of the kernel function, and overfit control through the choice of a single regularization parameter (Lee and Verri, 2002). SVM uses a separating hyperplane to create a classifier. The solution is based only on data points at the margin, which are called Support Vectors. An optimal separating hyperplane that maximizes the margin between different classes can be found through a constrained optimization process. The data points are not necessarily linearly separable. SVM can be used to classify data points that cannot be separated linearly by choosing a proper non-linear kernel function to generate a non-linear separating hyperplane and by incorporating an error tolerance factor (Vojislav, 2001).

An SVM was adopted as the classifier and the selected PC bands were sent to SVM for the training and classification. The MATLAB SVM toolbox (Gunn, 1998) was used for the classification. There are several parameters of the SVM to be set, such as the penalty parameter C in non-separable cases and the kernel function and its coefficient(s). In non-separable cases, there is a need to determine the extent of the tolerance to classification errors, i.e., to define a proper C value. The kernel function determines the type of separating hyperplane, which can substantially affect the classifier performance. These setting parameters need to be selected and adjusted properly for a SVM classifier to achieve a desired performance.

The experiments were done for the classification of AF13 and the three non-aflatoxin-producing *A. flavus* strains. According to the preliminary classification results (AF13, AF38) was the most difficult pair to classify compared with the other two pairs. Therefore, the SVM settings were determined by comparing the classification results of this pair. After comparing the classification results of using 17 different kernel functions in conjunction with five typical C values, the combination of using a third order polynomial kernel function with a C value of 3000 was chosen for training an SVM classifier (Fig. 3).

2.8. Training and testing with K-fold cross-validation

K-fold cross-validation (Kohavi, 1995) was used for training and testing. In K-fold cross-validation, the sample data was partitioned into K groups, and the training-testing process was repeated for K times. For each time, a single group was retained for testing, and the remaining $(K-1)$ groups were used as training data. Finally each of the K groups was used exactly once as the validation data. The advantage of K-fold cross-validation over repeated random sub-sampling validation was that all observations were used for both training and validation, and each observation was used for validation exactly once.

In this application 1800 pixels were selected for the K-fold cross-validation, among which 900 pixels were from AF13 and there were

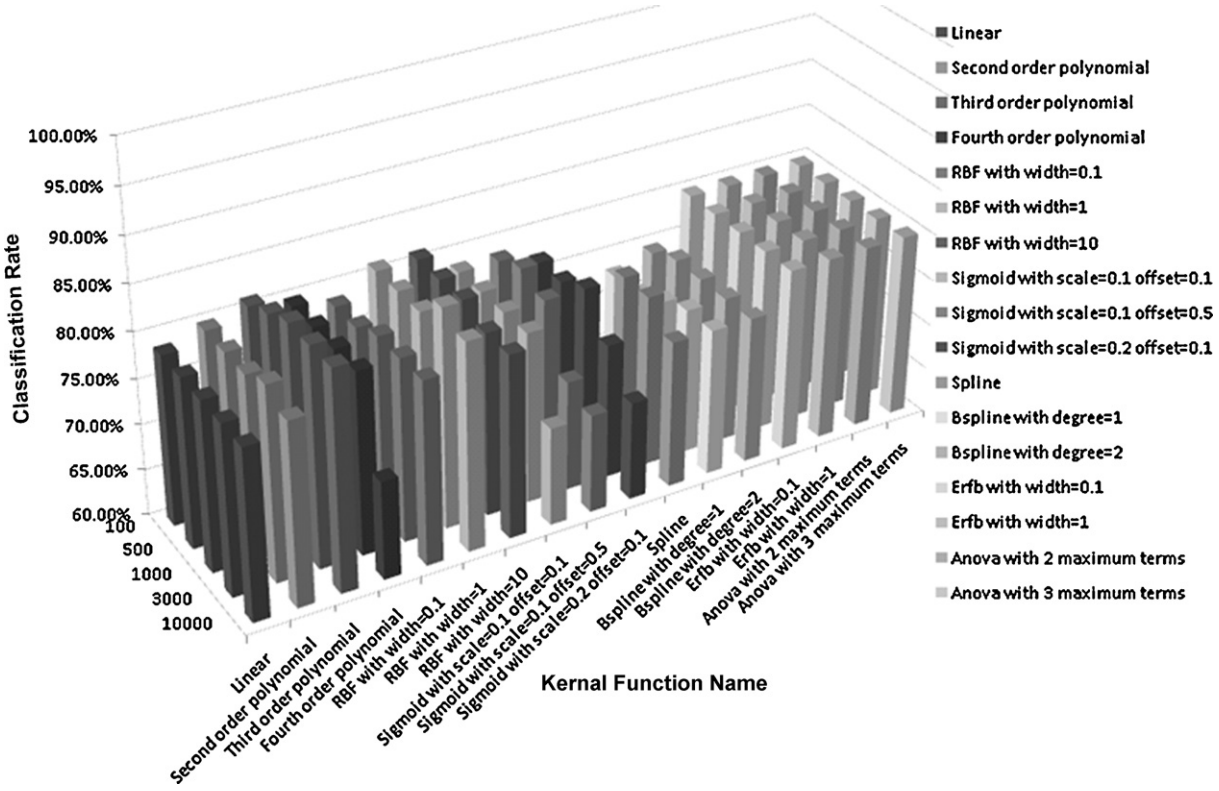

Fig. 3. Average classification rates between AF13 and AF38 with 17 different kernel functions and five different *C* values (under halogen light source).

300 pixels from each of the three non-toxigenic *A. flavus* strains. The 1800 pixels were divided into 12 folds, so that each fold had 75 pixels from AF13, and 25 pixels from each of the three atoxigenic strains. The validation process was repeated for 12 times. Each time one of the 12 folds was used for testing and the remaining 11 folds were used as training data sets. During training, an optimal separating hyperplane for the training set was determined. The trained SVM classifier was then used to classify the pixels in the testing sets. The classification results were collected and used for determining whether the toxigenic *A. flavus* was distinguishable from atoxigenic *A. flavus* by using the developed SVM classifier.

The *K*-fold cross-validation was also applied between AF13 and each specific atoxigenic *A. flavus*. For each pair of species, 600 pixels were selected from each species, and they were divided into 12 folds so there were 100 pixels in each fold.

The classification of each of the four species from the others was investigated. To do this, the "one-against-one" multi-class classification technique (Hsu and Lin, 2001) was adopted. In this research, there were $4 \times (4-1)/2 = 6$ pairs of classes and a classifier was constructed for each pair. Then, a "voting approach" was employed, which classified a pixel to the class having the largest number of votes. If two classes had the same number of votes, the final winner was chosen according to the SVM's classification result between these two classes.

Table 1
MANOVA *P*-values (with *F* values) of MANOVA for the pixels from three replicates of each AF strain.

Strain type	*P*-values (Halogen)	*P*-values (UV)
AF13	0.6220 ($F_{368,828} = 0.9398$)	0.4854 ($F_{368,828} = 0.9853$)
AF38	0.3610 ($F_{368,828} = 1.0333$)	0.1419 ($F_{368,828} = 1.1023$)
AF283	0.5152 ($F_{368,828} = 0.9743$)	0.4218 ($F_{368,828} = 1.0097$)
AF2038	0.6437 ($F_{368,828} = 0.9341$)	0.6557 ($F_{368,828} = 0.9411$)

3. Results

MANOVA was done in JMP 7.0.2 (SAS Institute Inc.). The resulting MANOVA *P*-values for the pixels from three replicates of each AF strain indicated no evidence of significant differences between means of the data from the three replicates was found for all AF strains (Table 1).

During PCA, the 'Scree Plot' of the PCs in the classification experiment between classes AF13 and AF38 under halogen light was generated (Fig. 4). The first PC explained about 43% of the total variance. But to explain up to 95% of the total variance, the first 40 PCs needed to be used.

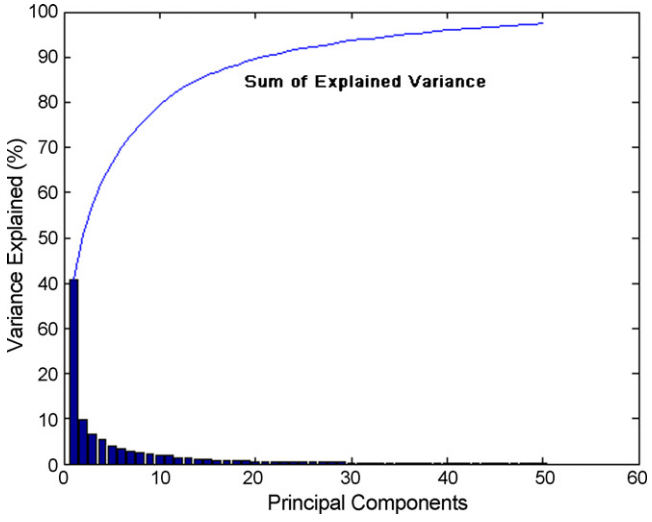

Fig. 4. 'Scree Plot' of principal components shows that to explain up to 95% of the total variance, the first 40 PCs needed to be used.

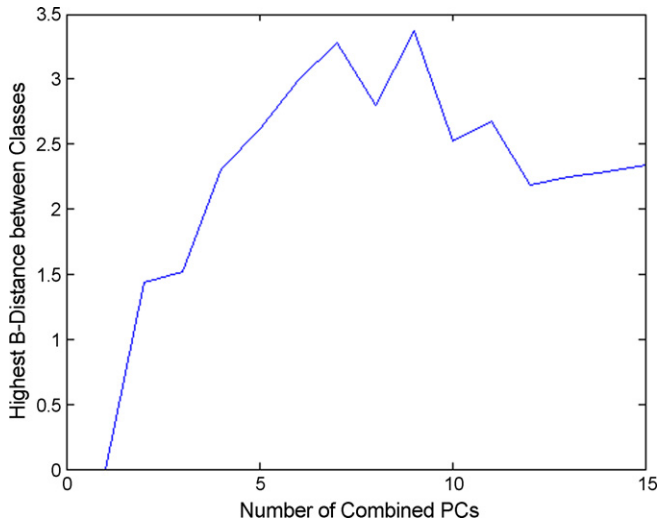

Fig. 5. Highest B-Distances of combinations of different numbers of PC bands resulted from greedy search among the 15 lowest order PCs for (AF13, AF38) under halogen light.

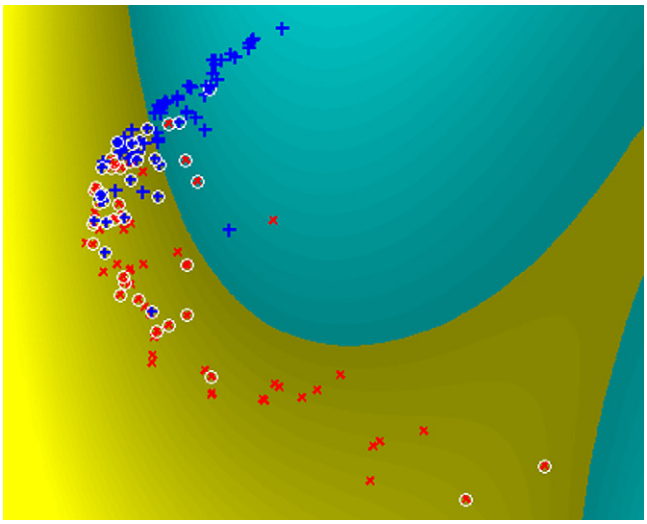

Fig. 6. An example of the training data and the trained classifier between toxigenic and atoxigenic fungus species. The '×'s are the toxigenic data points projected on the plane defined by the first two selected PCs. The blue '+'s are the atoxigenic data points projected on the same plane. The SVM separating function divided the space into two areas represented by different colors (blue and yellow). The circled points are the Support Vectors. (For interpretation of the references to color in this figure legend, the reader is referred to the web version of the article.)

Greedy search was first applied to find the combination of PCs leading to the maximum B-Distance between classes among the 15 lowest order PCs. Take the pair of classes AF13 and AF38 under halogen light as an example, a combination of 9 PCs was found with a B-Distance of 3.3719 between classes (Fig. 5).

For searching among the first 40 PCs (which explain more than 95% of the total variance), Genetic Algorithm (GA) was implemented instead of greedy search. For the same example of (AF13, AF38) under halogen light, GA found a combination of 9 PCs (the 1st, 2nd, 3rd, 5th, 6th, 13th, 21st, 23rd, 28th PCs) among the first 40 PCs with a B-Distance of 3.4906 after less than 200 generations of evolution within 2 min. This result was a further improved combination than the result of greedy search. This result was far better than the B-Distance produced by using all the 9 lowest order PCs, which was only 1.8101.

The PCs selected by GA were sent to SVM for the training and testing between the toxigenic and atoxigenic fungus species. The averaged classification accuracies of the 12-fold cross-validation are presented in Table 2. Under halogen light, 83% of toxigenic species and 74% of the atoxigenic species were classified correctly, while under UV light, 67% of toxigenic species and 85% of the atoxigenic species were classified correctly. One example of the training data and the trained SVM classifier is displayed in Fig. 6. According to the result above, SVM was an effective method for distinguishing toxigenic and atoxigenic species.

For the classification between the toxigenic fungus species AF13 and each specific atoxigenic fungus species (AF38, AF283 or AF2038), the averaged classification accuracies of the 12-fold cross-validation are presented in Tables 3–5. Accordingly, in average, 80% of the pixels were classified correctly for the pair (AF13, AF38) under halogen light sources. The classification accuracies for the other pairs were 91% for (AF13, AF283) and 95% for (AF13, AF2038) under halogen light sources, and 75% for (AF13, AF38), 97% for (AF13, AF283) and 99% for (AF13, AF2038) under UV lights. Therefore, AF13 was distinguishable from each specific atoxigenic fungus species under both lighting resources.

Though it has been shown that the toxigenic AF13 is distinguishable from the three atoxigenic fungus species AF38, AF283 and AF2038, it is also interesting to know whether each of the four species is distinguishable from the others. The multi-class classification was applied for this purpose. The classification accuracies are listed in Table 6. Under halogen light sources, 84% of AF13 pixels, 79% of AF38 pixels, 75% of AF283 pixels and 92% of AF2038 pixels were correctly classified, while under UV light sources, 82% of AF13 pixels, 97% of AF38 pixels and 100% of AF283 and AF2038 pixels were correctly classified. Based on the result, SVM was effective in distinguishing each fungus species from the others.

In general, high classification accuracies were achieved by SVM though there were variances among the results. Specifically, the classification rates of fungi under UV exposure were higher than that of those under halogen light exposure, except for the pair (AF13, AF38). It is also noteworthy that under the UV light source,

Table 2
The average classification accuracies between toxigenic and atoxigenic fungus species.

	Toxigenic (Halogen)	Atoxigenic (Halogen)	Toxigenic (UV)	Atoxigenic (UV)
Classified as toxigenic	83%	26%	67%	15%
Classified as atoxigenic	17%	74%	33%	85%

Table 3
The average classification accuracies between AF13 and AF38.

	AF13 (Halogen)	AF38 (Halogen)	AF13 (UV)	AF38 (UV)
Classified as AF13	82%	21%	69%	20%
Classified as AF38	18%	79%	31%	80%

Table 4
The average classification accuracies between AF13 and AF283.

	AF13 (Halogen)	AF283 (Halogen)	AF13 (UV)	AF283 (UV)
Classified as AF13	96%	15%	97%	2%
Classified as AF283	4%	85%	3%	98%

Table 5
The average classification accuracies between AF13 and AF2038.

	AF13 (Halogen)	AF2038 (Halogen)	AF13 (UV)	AF2038 (UV)
Classified as AF13	90%	0%	99%	0%
Classified as AF2038	10%	100%	1%	100%

Table 6
The multi-class classification accuracies for each fungus species (under halogen light source).

Light source	Halogen	Halogen	Halogen	Halogen	UV	UV	UV	UV
Fungus	AF13	AF38	AF283	AF2038	AF13	AF38	AF283	AF2038
Classified as AF13	84%	2%	8%	1%	82%	3%	0%	0%
Classified as AF38	11%	79%	12%	4%	17%	97%	0%	0%
Classified as AF283	0%	16%	75%	4%	1%	0%	100%	0%
Classified as AF2038	5%	3%	4%	92%	0%	0%	0%	100%

the average classification accuracies were above 95% for the pairs (AF13, AF283) and (AF13, AF2038). Besides, all 184 bands were used by this method and there was no feature (band) selection implemented yet. The implementation of feature selection has the potential to shorten the data collection time as well as to further improve the classification result. The investigation of the roles of different light sources and different bands in the classification process remains as future work.

4. Conclusions

Support Vector Machine was applied to classify hyperspectral image pixels of toxigenic and atoxigenic strains of *A. flavus*. Under halogen light sources, 83% of the toxigenic fungus pixels and 74% of the atoxigenic fungus pixels were correctly classified, while under UV light sources, 67% of the toxigenic fungus pixels and 85% of the atoxigenic fungus pixels were correctly classified. The pairwise classification accuracies between toxigenic AF13 and each atoxigenic fungus species (AF38, AF283 and AF2038) were 80%, 91% and 95% under halogen light sources, and 75%, 97% and 99% under UV lights, respectively. Based on the results, hyperspectral images of atoxigenic and toxigenic *A. flavus* can be classified by using SVM. Multi-class classification was applied to check if each fungus species was distinguishable from other three species. The results showed that (AF38, AF283) under halogen light source and (AF13, AF38) under UV light source were the pairs most difficult to classify. The classification results under halogen light source were compared with those under UV light source. Generally the classification accuracies with UV lights were higher. It is noteworthy that under the UV light source, the average pixel-wise classification accuracies were above 95% for the pairs (AF13, AF283) and (AF13, AF2038).

References

Adye, J., Mateles, R.I., 1964. Incorperation of labeled compounds into aflatoxins. Biochim. Biophys. Acta 86, 418–420.

Ariana, D., Guyer, D.E., Shrestha, B., 2006. Integrating multispectral reflectance and fluorescence imaging for defect detection on apples. Comput. Electron. Agric. 50 (2), 148–161.

Baird, R.E., Trigiano, R.N., Windham, G.L., Williams, W.P., Kelly, R., Abbas, H.K., Moulton, J.K., Scruggs, M.L., 2006. Comparison of aflatoxigenic and nonaflatoxigenic isolates of *Aspergillus flavus* using DNA amplification fingerprinting techniques. Mycopathologia 161, 93–99.

Bhattacharyya, A., 1943. On a measure of divergence between two statistical populations defined by probability distributions. Bull. Calcutta Math. Soc. 35, 99–109.

Cheng, X., Chen, Y.R., Tao, Y., Wang, C.Y., Kim, M.S., Lefcourt, A.M., 2004. A novel integrated PCA and FLD method on hyperspectral image feature extraction for cucumber chilling damage inspection. Trans. ASAE 47 (4), 1313–1320.

Davis, N.D., Iyer, S.K., Diener, U.L., 1987. Improved method of screening for aflatoxin with a coconut agar medium. Appl. Environ. Microbiol. 53, 1593–1595.

De, J., Kenneth, A., 1975. Analysis of the behavior of a class of genetic adaptive systems. Ph.D. thesis. Computer and Communication Science Dept., University of Michigan, Ann Arbor, MI.

DiCrispino, K., Yao, H., Hruska, Z., Brabham, K., Lewis, D., Beach, J., Brown, R.L., Cleveland, T.E., 2005. Hyperspectral imagery for observing spectral signature change in *Aspergillus flavus*. Optical sensors and sensing systems for natural resources and food safety and quality. Proc. SPIE 5996, 45–53.

Duda, R.O., Hart, P.E., 1973. Pattern Classification and Scene Analysis. John Wiley & Sons, New York.

Dyer, S.K., McCammon, S., 1994. Detection of toxigenic isolates of *Aspergillus flavus* and related species on coconut cream agar. J. Appl. Bacteriol. 76, 75–78.

Goldberg, D.E., 1989a. Genetic Algorithms in Search, Optimization and Machine Learning. Addison-Wesley Publishing Co., Inc., Reading.

Goldberg, D.E., 1989b. Sizing populations for serial and parallel genetic algorithms. In: Proceedings of the Third International Conference on Genetic Algorithms, San Mateo, CA, pp. 70–79.

Gordon, S.H., Wheeler, B.C., Schudy, R.B., Wicklow, D.T., Greene, R.V., 1998. Neural network pattern recognition of photoacoustic FTIR spectra and knowledge-based techniques for detection of mycotoxigenic fungi in food grains. J. Food Protect. 61 (2), 221–230.

Gordon, S.H., Jones, R.W., McClelland, J.F., Wicklow, D.T., Greene, R.V., 1999. Transient infrared spectroscopy for detection of toxigenic fungi in corn: potential for on-line evaluation. J. Agric. Food Chem. 47, 5267–5272.

Greene, R.V., Gordon, S.H., Jackson, M.A., Bennett, G.A., 1992. Detection of fungal contamination in corn: potential of FTIR-PAS and -DRS. J. Agric. Food Chem. 40, 1144–1149.

Gunn, S.R., 1998. Support Vector Machines for Classification and Regression. University of Southampton.

Guyer, D., Yang, X., 2000. Use of genetic artificial neural networks and spectral imaging for defect detection on cherries. Comput. Electron. Agric. 29 (3), 179–194.

Hruska, Z., Yao, H., DiCrispino, K., Brabham, K., Lewis, D., Beach, J., Brown, R.L., Cleveland, T.E., 2005. Hyperspectral imaging of UVR effects on fungal spectrum. Proc. SPIE 5886, 273–283.

Hsu, C.W., Lin, C.J., 2001. A Comparison of Methods for Multi-class Support Vector Machines. Technical Report. Department of Computer Science and Information Engineering, National Taiwan University, Taipei, Taiwan.

Hwang, J., Lay, S., Lippman, A., 1994. Nonparametric multivariate density estimation: a comparative study. IEEE Trans. Signal Process. 42 (10), 2795–2810.

Kohavi, R., 1995. A study of cross-validation and bootstrap for accuracy estimation and model selection. In: Proceedings of the Fourteenth International Joint Conference on Artificial Intelligence, vol. 2 (12), pp. 1137–1143.

Lee, S.W., Verri, A., 2002. Pattern recognition with support vector machines. In: Proceedings of the First International Workshop, SVM 2002, Niagara Falls, Canada, August 10. Springer, Heidelberg, Lecture Notes in Computer Science 2388.

Luis, J., Landgrebe, D., 1998. Supervised classification in high dimensional space: geometrical statistical and asymptotical properties of multivariate data. IEEE Trans. Syst. Man Cybern. 28 (1), 39–54.

Pearson, K., 1901. On lines and planes of closest fit to systems of points in space. Philos. Mag. 2 (6), 559–572.

Pearson, T.C., Wicklow, D.T., 2001. Detecting aflatoxin in single corn kernels by transmittance and reflectance spectroscopy. Trans. ASAE 44 (5), 1247–1254.

Reyes-Aldasoro, C.C., Bhalerao, A., 2006. The Bhattacharyya space for feature selection and its application to texture segmentation. Pattern Recogn. 39 (5), 812–826.

Scott, D.W., 1992. Multivariate Density Estimation. John Wiley & Sons, New York.

Tang, L., Tian, L.F., Steward, B.L., 2000. Color Image segmentation with genetic algorithm for in-field weed sensing. Trans. ASAE 43, 1019–1027.

Torrey, G.S., Marth, E.H., 1976. Silica gel medium to detect molds that produce aflatoxin. Appl. Environ. Microbiol. 32, 376–380.

USDA, 2002. Aflatoxin Handbook. United States Department of Agriculture, Grain Inspection, Packers and Stockyards Administration, Washington, DC.

Vapnik, V.N., 1995. The Nature of Statistical Learning Theory. Springer-Verlag New York, Inc., New York.

Vojislav, K., 2001. Learning and Soft Computing, Support Vector Machines, Neural Networks, and Fuzzy Logic Models. The MIT Press, Cambridge.

Yao, H., Tian, L.F., Kaleita, A., 2003. Hyperspectral image feature extraction and classification for soil nutrient mapping. In: Stafford, J., Werner, A. (Eds.), Proceeding of Fourth European Conference on Precision Agriculture. Wageningen Academic Publishers, Wageningen.